

AMSI **VACATIONRESEARCH**
SCHOLARSHIPS 2022–23

*SET YOUR SIGHTS ON
RESEARCH THIS SUMMER*



Knots and Combinatorics

Oscar Eden

Supervised by Daniel Mathews and Jian He
Monash University

Contents

1	Prelude	2
1.1	Acknowledgements	2
1.2	Abstract	2
1.3	Statement of Authorship	2
2	Introduction	2
3	Triangulations of Knot Complements	3
3.1	Manifolds and Knots	3
3.2	Triangulations of Knot Complements	4
3.2.1	Figure-8 Knot Complement Triangulation	4
4	Some Hyperbolic Geometry	7
4.1	Hyperbolic 2-space	7
4.2	Hyperbolic 3-space	8
4.3	Geometric structures and gluing equations	8
4.3.1	Geometric triangulations	9
4.3.2	Gluing equations	9
5	Cusp Homology and Peripheral Curves	11
6	Tetrahedron Index	11
7	3D Index	12
7.1	Incidence and Neumann-Zagier Matrices	12
7.2	Evaluation of the 3D Index	13
7.2.1	3D Index With no Peripheral Curves	13
7.2.2	Evaluation for a Single Torus Boundary Component With Peripheral Curves	13
7.2.3	Evaluation for Multiple Tori Boundary Components With Peripheral Curves	14
7.3	Example Calculations	14
7.3.1	Figure-8 Knot	15
7.3.2	5 ₂ Knot	15
8	Discussion and Conclusion	16
9	Appendix	17
9.1	Locally Euclidean Requirements.	17
9.2	Equivalence of knots.	18
9.3	Polyhedron definition	18

9.4	Relating Hyperbolic and Riemannian Geometry	18
9.5	Definition of Geometric Structure	19
9.6	Proof of Equivalence Between the Numbers of Tetrahedra and Edge Classes	19
9.7	Properties of the tetrahedron index I_{Δ}	19
9.8	Proof of the Invariance of J_{Δ} under S_3	20

1 Prelude

1.1 Acknowledgements

1.2 Abstract

1.3 Statement of Authorship

2 Introduction

Knot theory is subfield a topology and is concerned with the study of mathematical knots [1]. A mathematical knot is closely related to our intuitive notation of a knot, except when forming mathematical knots we tangle the piece of string and then glue its ends together. Knots have long been objects of intrigued appearing in Tibetan Buddhism and in the books of Celtic monks [1]. Moreover techniques from knot theory have found uses in many other parts of science such as DNA modelling, statistical mechanics and string theory [1].

One can also ask interesting questions about knots such as which knots are the same. This led to the development of quantities called knot invariants which are tools which allow us to tell knots apart (most do not tell whether two knots are the same, although some do and these are called complete knot invariants). There are a variety of knot invariants such as crossing number which associates an integer to a knot, corresponding to the minimum number of crossings for the knot, or more complex examples such as the Jones polynomial which is a polynomial computed from properties of the knot.

In this report we will focus on an object called the 3D index which is a invariant of 3-manifolds with torus boundary components. The 3D index originally arose out of the work of three physicists Dimofte, Gaiotto and Gukov, who were studying three-dimensional $N = 2$ superconformal field theories [2]. Note the prefix of super in superconformal refers to supersymmetry which is a theoretical (meaning it has not been observed) symmetry between the fermions (matter particles) and the bosons (the force particles) in the standard model.

Broadly speaking, for some 3-manifold with r number of tori boundary components the 3D index is a collection of formal power series in the variable $q^{\frac{1}{2}}$, with each power series in this collection corresponding to some peripheral curve on the boundary of the 3-manifold. The 3D index is not a completely well-defined function as the coefficients in the formal power series are not guaranteed to converge and it can only be calculated using a suitable triangulation of the manifold [3], [4]. A triangulation of a 3-manifold is a collection of ideal tetrahedra (tetrahedra with their vertices removed) and a gluing (here a gluing means a particular procedure for gluing the

faces, edges and ideal vertices of the ideal tetrahedra) [5], [6]. In this report we will discuss further a general procedure for obtaining these triangulations for 3-manifolds (or more specifically knot complements).

Further the manner in which this gluing occurs can be stored in a matrix called the incidence matrix. Also when working with geometric ideal triangulations where the ideal tetrahedra now have additional hyperbolic structure the gluing can be described by gluing equations which can be encoded via the Neumann-Zagier matrix (which can be derived from the incidence matrix) [7]. In this report we wrote a MATLAB function which for any knot complement with a single torus boundary this function would take in an incidence matrix for some triangulation and a peripheral curve (described by its homology class) and return the corresponding 3D index.

3 Triangulations of Knot Complements

3.1 Manifolds and Knots

Before considering objects in some space, such as knots in Euclidean 3-space, we should first give a definition of a space (or more precisely a manifold).

Definition 3.1. An n -manifold M is Hausdorff, second-countable and locally Euclidean. The exact requirements of the locally Euclidean condition depends on the category we are working and can be found in the appendix.

With the notion of a manifold in hand we will give the mathematically rigorous definition of the central objects in knot theory.

Definition 3.2. A knot $K \subset S^3$ is a set which is homeomorphic to a circle S^1 in S^3 . An object which generalises a knot is a link which is a subset of S^3 that is PL or smooth homeomorphic to a disjoint union of any number of S^1 circles. Also just as for knots a link can be defined as a PL or smooth embedding $L : S^1 \sqcup \dots \sqcup S^1 \rightarrow S^3$.

Alternatively we can view knots and links as embeddings will lead to the definition.

Definition 3.3. A knot K is an embedding (in other words an injective map) $K : S^1 \rightarrow S^3$. Also a link can be defined as an embedding $L : S^1 \sqcup \dots \sqcup S^1 \rightarrow S^3$.

But with this definition of K as an embedding we see that these two definitions are complementary as the earlier definition can be seen as the image of the embedding given by the latter definition. Thus, we will simply refer to both the embedding and its image as K . Moreover now that we have mathematically grounded our idea of a knot, an interesting question is how we define when knots are the same which is defined in the appendix.

Knots are visualised via knot diagrams.

Definition 3.4. A knot diagram is a 4-valent graph with over and under crossing information at each vertex. The diagram is embedded in a plane $S^2 \subset S^3$ called the projection plane.

For any knot we can find a solid tubing around that knot, which is called a regular tubular neighbourhood.

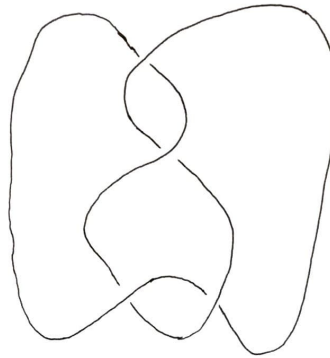


Figure 1: Knot diagram of the figure-8 knot.

Theorem 3.5. *For any knot $K \subset S^3$ there exists a regular tubular neighbourhood of K , thus there is an embedding of the solid torus $S^1 \times D^2$ into S^3 such that $S^1 \times \{0\}$ maps to K [5].*

We can now define two types of manifolds which will serve as important objects of study in this report.

Definition 3.6. Let K be a knot then it has some open regular neighbourhood which we call $N(K)$. The knot exterior is the manifold defined as $S^3 - N(K)$, note this is a compact 3-manifold with torus boundary. While the knot complement is the open manifold defined as $S^3 - K$ which is homeomorphic to the interior of the knot exterior. Analogous manifolds also exist for links.

3.2 Triangulations of Knot Complements

To build triangulations we must first introduce the objects that make up triangulations.

Definition 3.7. An ideal polyhedron is a polyhedron with all its vertices removed.

Then we define triangulations as follows.

Definition 3.8. Let M be a 3-manifold. An ideal triangulation of M is a combinatorial way of gluing ideal tetrahedra such that the result is homeomorphic to M . Note the gluing should take faces to faces, edges to edges, etc.

The reason for the existence of triangulations is that manifolds can be quite complex objects, but they can be simplified through viewing them as the gluing together of simpler objects.

3.2.1 Figure-8 Knot Complement Triangulation

There is a general procedure for finding a triangulation of any link complement [6]. We will give a rough outline of this procedure using the knot complement of the figure-8 knot. First we draw the knot diagram (given by

Figure 1) and then we can think of the two polyhedra in the decomposition as each corresponding each to a balloon. One of the balloons expands from below the diagram and the other expands from above the diagram.

The two balloons will come into contact in the regions of the plane which are outlined by the knot diagram, and we labelled these regions as they will be the faces of the polyhedra. Moreover as the balloons expand further we see that the faces intersect along edges corresponding to crossings. There is an edge for each crossing and we give the edge orientation by making it run from the top to the bottom (equally we could chosen the opposite orientation).

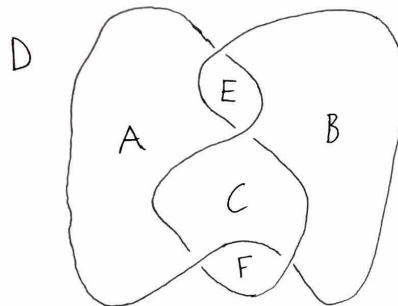


Figure 2: Knot diagram of the figure-8 knot with labelled faces.

This is the geometric intuition for the combinatorial method we will outline below following Purcell's hyperbolic knot theory [5].

Step 1: Sketch faces and edges into the diagram.

As described earlier we start with knot diagram and label the faces corresponding the regions cut out by the knot diagram. We should note that the unbounded region also corresponds to a face. Further we mentioned that edges arise as the result of arcs which connect the two strands at a crossing, these are called crossing arcs. At each crossing on the knot diagram we draw four arcs (all with the same orientation) and it is clear that each of these arcs are ambient isotopic in S^3 to each other. The motivation for drawing the four edges is that it makes it clear which edges bound particular faces of the polyhedra. Also label the edges which are ambient isotopic (using ticks).

Step 2: Shrink the knot to ideal vertices on the top polyhedron.

At this point we should be reminded that we are interested in the knot complement $S^3 - K$, and so given that the edges start on the knot and end on the knot, we see that the edge must be an ideal edge (does not have vertices). Therefore given that the knot is not part of the manifold $S^3 - K$ we will now shrink the strands of the knot. The strands are shrunk by retracting each strand to a single point. As we are considering the knot complement, the complement of the strand on the boundary of the ball is homeomorphic to the complement of a single point on the boundary of the ball. Thus we can replace strands with ideal vertices (single removed points).

So turning our attention back to the top polyhedron. When considering the top polyhedron we can identify the two edges which are isotopic along an overstrand, but we can't identify the two edges which are isotopic

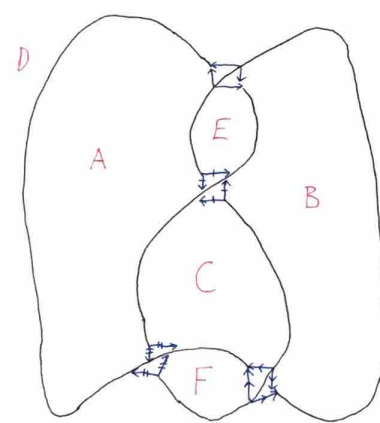


Figure 3: Figure-8 knot with crossing arcs.

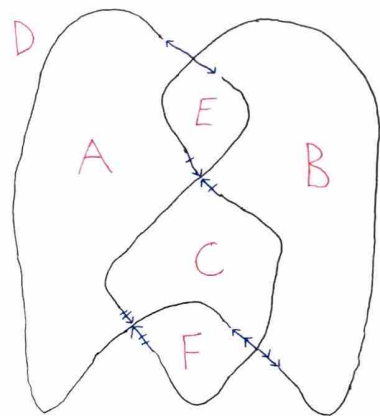


Figure 4: Figure-8 knot complement with isotopic edges identified.

along understrands. From inside the top polyhedron the visible components of the knot are the overstrands. Moreover we see that a crossing, the understrand ends in an edge while the overstrand continues on and passes the same edge twice (once on each side). Hence once we identify each overstrand to a single ideal vertex we end up with a pattern of faces, edges and ideal vertices describing the top polyhedron.

Step 3: Shrink the knot to ideal vertices on the bottom polyhedron.

If instead of viewing the knot diagram from above we viewed it from the opposite (or below) then the overstrands would become understrands and the understrands would be overstrands. So now perform an analogous procedure to that described above where still viewing the knot diagram from above we identify the edges that are isotopic via sliding an endpoint along an understrand on the bottom polyhedron. Then we shrink each knot component corresponding to an understrand to an ideal vertex, and this gives the bottom polyhedron as a sequence of faces, edges and ideal vertices.

Thus we have obtained a decomposition of $S^3 - K$ into ideal polyhedra.

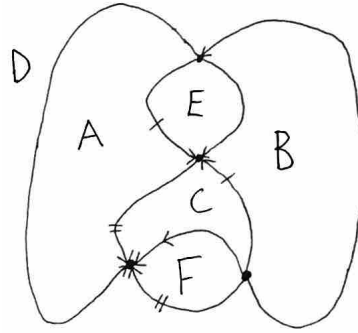


Figure 5: The top ideal polyhedron viewed from inside.

4 Some Hyperbolic Geometry

Hyperbolic geometry is a non-Euclidean geometry which replaces the Euclidean 'parallel axiom' that if \mathbf{p} is a point that is not on a straight line l then there is a unique straight line passing through \mathbf{p} that does not intersect l , with that if \mathbf{p} is a point that is not on a straight line l then there is at least two straight lines passing through \mathbf{p} which does not intersect l .

4.1 Hyperbolic 2-space

There are many models of hyperbolic spaces, such a model corresponding to hyperbolic 2-space \mathbb{H}^2 is the upper half-plane model. For this model we define that

$$\mathbb{H}^2 = \{x + iy \in \mathbb{C} | y > 0\} = \{z \in \mathbb{C} | \text{Im}(z) > 0\},$$

with a metric whose first fundamental form is given by

$$ds^2 = \frac{dx^2 + dy^2}{y^2}.$$

Now with this specific model of hyperbolic geometry we can relate it to the more general idea of Riemannian geometry, which is done in the appendix.

Definition 4.1. The boundary at infinity of \mathbb{H}^2 is defined to be $\mathbb{R} \cup \{\infty\}$ it is homeomorphic to S^1 and denoted by S_∞^1 , $\partial\mathbb{H}^2$ or $\partial_\infty\mathbb{H}^2$.

Definition 4.2. An isometry between Riemannian manifolds M and N is a diffeomorphism $f : M \rightarrow N$ such that $\langle v, w \rangle_p = \langle D_p f(v), D_p f(w) \rangle_{f(p)}$ for any $p \in M$ and $v, w \in T_p M$.

Isometries have the nice property that they preserve many geometric quantities such as lengths and angles. If we consider the set of orientation preserving isometries from \mathbb{H}^2 to itself this forms a group.

Theorem 4.3. The full group of isometries of \mathbb{H}^2 is generated by reflections in geodesics in \mathbb{H}^2 . The group of orientation preserving isometries of \mathbb{H}^2 is the group of linear fractional transformations

$$z \mapsto \frac{az + b}{cz + d},$$

where $a, b, c, d \in \mathbb{R}$ and $ad - bc > 0$.

4.2 Hyperbolic 3-space

With the development of two dimensional hyperbolic space we can also define hyperbolic 3-space as

$$\mathbb{H}^3 = \{(x + iy, t) \in \mathbb{C} \times \mathbb{R} | t > 0\}$$

under the metric with first fundamental form

$$ds^2 = \frac{dx^2 + dy^2 + dt^2}{t^2}.$$

The group $PSL(2, \mathbb{C})$ is the group of projective 2 by 2 matrices with complex coefficients and determinant 1.

Theorem 4.4. *The full group of isometries of \mathbb{H}^3 is generated by reflections in geodesic planes. The group of orientation preserving isometries of \mathbb{H}^3 is $PSL(2, \mathbb{C})$. Its action on the boundary $\partial\mathbb{H}^3 = \mathbb{C} \cup \{\infty\}$ is the usual action of $PSL(2, \mathbb{C})$ on $\mathbb{C} \cup \{\infty\}$, via Mobius transformation.*

Any element $A \in PSL(2, \mathbb{C})$ can be represented by a matrix up to multiplication by $\pm Id$. Then the action of,

$$A = \pm \begin{pmatrix} a & b \\ c & d \end{pmatrix}$$

on $\partial\mathbb{H}^3$ is defined to be

$$A(z) = \frac{az + b}{cz + d},$$

for $z \in \partial\mathbb{H}^3$.

Definition 4.5. An ideal tetrahedron in \mathbb{H}^3 is a tetrahedron in \mathbb{H}^3 with all four vertices on $\partial\mathbb{H}^3$, and with geodesic edges and faces.

As there exists a Mobius transformation taking any three points in $\mathbb{C} \cup \{\infty\}$ to 0, 1 and ∞ , we can as a result assume that the four vertices of the tetrahedron are positioned at 0, 1, ∞ and some $z \in \mathbb{C} \setminus \{0, 1\}$. This z parameterises the tetrahedron.

4.3 Geometric structures and gluing equations

A technical definition of geometric is given in the appendix, but it ultimately leads to the following definition of hyperbolic manifolds.

Definition 4.6. When a n -manifold admits a $(\text{Isom}(\mathbb{H}^n), \mathbb{H}^n)$ -structure we say that the manifold admits a hyperbolic structure or is simply hyperbolic.

4.3.1 Geometric triangulations

Definition 4.7. Let M be a 3-manifold, then a topological ideal triangulation of M is a combinatorial way of gluing ideal tetrahedra such that the result is homeomorphic to M . The truncated parts of the tetrahedra will correspond to the boundary of M .

Building on the earlier method of finding an ideal triangulation for a knot complement, Purcell outlines how to obtain a topological ideal triangulation from the ideal triangulation [5].

Firstly we start with an ideal triangulation and choose some ideal vertex v to cone to. The meaning of coning to v is that we add edges between this ideal vertex and all other ideal vertices (for which an edge does not already exist). Then for any two edges meeting at v we add an ideal triangle, and it should be noted that this might require an additional edge opposite v to be added. With these ideal triangles added, between any three ideal triangles meeting v we add an ideal tetrahedron. The resulting tetrahedra are then split off, and this reduces the collection of ideal polyhedra to a collection with at least one fewer ideal vertices. Thus by performing this procedure a finite number of times we obtain a topological ideal triangulation for the knot complement.

Definition 4.8. Let M be a 3-manifold, then a geometric ideal triangulation of M is a topological ideal triangulation such that each tetrahedron has a (positively oriented) hyperbolic structure, and the result of the gluing is a smooth manifold with a complete metric.

4.3.2 Gluing equations

A general fact regarding the gluing of hyperbolic polygons is the following.

Theorem 4.9. *A gluing of hyperbolic polygons gives a 2-manifold with a hyperbolic structure if and only if for each finite vertex v of the polygons, the sum of interior angles at each vertex glued to v is 2π .*

A similar fact can be found for gluing hyperbolic tetrahedra.

Definition 4.10. Let T be an ideal tetrahedron embedded in \mathbb{H}^3 and take some edge e on the tetrahedron. Then we can choose some isometry of \mathbb{H}^3 taking the endpoints of e to 0 and ∞ , as well as sending some other vertex to $1 \in \mathbb{C}$. The choice of these three points uniquely defines an isometry of \mathbb{H}^3 . The fourth vertex of the tetrahedron T will be mapped to some $z' \in \mathbb{C}$ and we can assume that z' has positive imaginary part, since if not we can apply an isometry rotating around the geodesic from 0 to ∞ which takes z' to 1 and takes the vertex at 1 to a complex number with positive imaginary component. Therefore we define $z(e) \in \mathbb{C}$ to be the complex number with positive imaginary part obtained by applying the unique isometry of \mathbb{H}^3 that takes the vertices of e to 0 and ∞ , and another vertex to 1, and call $z(e)$ the edge invariant of e .

It can be shown that the edge invariants of an ideal tetrahedron are related in the following way.

Lemma 4.11. *Let T be an ideal tetrahedron with edge e_1 , mapped such that the endpoints of e_1 lie at 0 and ∞ and the other vertices are located at 1 and $z(e_1)$. Then T has the following edge invariants.*

The edge e'_1 opposite e_1 , with vertices 1 and $z(e_1)$ has edge invariant $z(e'_1) = z(e_1)$.

The edge e_2 with vertices ∞ and 1 has edge invariant

$$z(e_2) = \frac{1}{1 - z(e_1)}.$$

Finally, the edge e_3 with vertices ∞ and $z(e_1)$ has edge invariant

$$z(e_3) = \frac{z(e_1) - 1}{z(e_1)}.$$

Therefore we obtain the following relationships,

$$z(e_1)z(e_2)z(e_3) = -1,$$

and

$$1 - z(e_1) + z(e_2)z(e_3) = 0.$$

So now we turn our minds to gluing ideal tetrahedra. First fix an edge of the gluing which we will call e and let T_1 be an ideal tetrahedron with edge e_1 glued to e . If we map T_1 in \mathbb{H}^3 such that e_1 runs from 0 and ∞ and a third vertex at 1, then the fourth vertex is at $z(e_1)$. Let F_1 be the face of T_1 with vertices 0, ∞ and $z(e_1)$, then this face is glued to a face F'_1 on some ideal tetrahedron T_2 . Also we denote the edge e_2 of T_2 which glues to e .

Since we're gluing to T_1 we want F'_1 to have vertices 0, ∞ and $z(e_1)$. Hence, for the gluing we apply the isometry to \mathbb{H}^3 fixing 0, ∞ and mapping 1 to $z(e_1)$, then under this mapping the fourth vertex of T_2 is mapped to $z(e_1)z(e_2)$.

We can continue this procedure of gluing ideal tetrahedra anti-clockwise. So the next tetrahedra will have vertices 0, ∞ , $z(e_1)z(e_2)$ and $z(e_1)z(e_2)z(e_3)$. Finally we'll eventually reach a final tetrahedra which is attached to T_1 , which will have vertices 0, ∞ , $z(e_1)z(e_2) \cdots z(e_{n-1})$ and $z(e_1)z(e_2) \cdots z(e_n)$.

With this method of gluing ideal tetrahedra in mind we can finally introduce the gluing equations, which follow directly from the earlier lemma giving the necessary and sufficient condition for when gluing hyperbolic polyhedra gives a hyperbolic manifold.

Theorem 4.12. *Let M admit a topological ideal triangulation such that each ideal tetrahedron has a hyperbolic structure. The hyperbolic structures on the ideal tetrahedra induce a hyperbolic structure on the gluing, M , if and only if for each edge e ,*

$$\prod z(e_i) = 1,$$

and

$$\sum \arg(z(e_i)) = 2\pi.$$

The above theorem gives the gluing equations which were discovered by William Thurston [7].

5 Cusp Homology and Peripheral Curves

Before introducing we need one more prerequisite.

Definition 5.1. Let M be a 3-manifold with torus boundary, then we define a cusp, or cusp neighbourhood of M to be a neighbourhood of ∂M homeomorphic to the product of a torus and an interval, $T^2 \times I$. Also it is defined that a cusp torus is a torus component of ∂M , or the boundary of a cusp.

Definition 5.2. Let M have a topological ideal triangulation. If we truncate the vertices of each ideal tetrahedron, we obtain a collection of triangles, each of which lies on the boundary of a cusp. Edges of each triangle inherit a gluing from the gluing of faces of the ideal tetrahedra. This gives a triangulation of each boundary torus, which we call a cusp triangulation.

Moreover in our calculations of the 3D index we will often have peripheral curves. A peripheral curve γ is an oriented multicurve on ∂M with no contractible components. It is possible to deform γ such it is in the normal form or position with respect to the triangulation $T_{\partial M}$ of ∂M that is induced by the ideal triangulation T of M . This means that γ is a disjoint union of oriented normal arcs in each triangle of $T_{\partial M}$, and a normal arc is a simple arc which connects two distinct sides of a triangle [8].

6 Tetrahedron Index

Definition 6.1. For an ideal triangulation the tetrahedron index is $I_{\Delta} : \mathbb{Z}^2 \rightarrow \mathbb{Z}[[q^{\frac{1}{2}}]]$,

$$I_{\Delta}(m, e) = \sum_{n=(-e)_{+}}^{\infty} (-1)^n \frac{q^{\frac{1}{2}n(n+1) - (n+\frac{1}{2}e)m}}{(q)_n (q)_{n+e}},$$

where $e_{+} = \max\{0, e\}$ and $(q)_n = \prod_{i=1}^n (1 - q^i)$ is a q-Pochhammer symbol [3]. We define $(q)_0 = 1$ and for $n < 0$ it is often taken by convention that $\frac{1}{(q)_n} = 0$.

Recall that the general formula for geometric power series is given by

$$\frac{1}{1 - q^n} = \sum_{i=0}^{\infty} q^{in} = 1 + q + q^2 + q^3 + \dots .$$

Thus the q-Pochhammer symbol can be written as,

$$\frac{1}{(q)_n} = \prod_{i=1}^n \frac{1}{1 - q^i} = \prod_{i=1}^n (1 + q^i + q^{2i} + \dots).$$

So we see that the tetrahedron index is a formal power series. We can calculate some examples (using code in the appendix),

$$I_{\Delta}(0, 0) = 1 - q - 2q^2 - 2q^3 - 2q^4 + q^6 + \dots .$$

$$I_{\Delta}(1, -1) = -q^{\frac{1}{2}} + q^{\frac{5}{2}} + 2q^{\frac{7}{2}} + 3q^{\frac{9}{2}} + \dots .$$

From its definition it is not obvious that the coefficients of the terms in the tetrahedron index should converge or that the exponents should all be non-negative, but in fact both of these are true [3]. The tetrahedron index also has a variety of other properties (which are located in the appendix) proven in [3].

It can be convenient to work with a variation of the tetrahedron index, which is defined for integers a, b, c as [4]

$$J_{\Delta}(a, b, c) = (-q^{\frac{1}{2}})^{-b} I_{\Delta}(b - c, a - b) = (-q^{\frac{1}{2}})^{-c} I_{\Delta}(c - a, b - c) = (-q^{\frac{1}{2}})^{-a} I_{\Delta}(a - b, c - a).$$

Immediately we see that this is a more symmetric notation for the tetrahedron index. Also it should be noted that the equalities $(-q^{\frac{1}{2}})^{-b} I_{\Delta}(b - c, a - b) = (-q^{\frac{1}{2}})^{-c} I_{\Delta}(c - a, b - c) = (-q^{\frac{1}{2}})^{-a} I_{\Delta}(a - b, c - a)$ are a consequence of the triality identity of I_{Δ} . Moreover $J_{\Delta}(a, b, c)$ is invariant under S_3 (in other words it's invariant under all permutations of its arguments a, b, c) and a proof is given in the appendix [4].

7 3D Index

Let T be an oriented ideal triangulation with n tetrahedra of a 3-manifold M with r tori boundary components. An Euler characteristic argument (given in the appendix) gives that the number of edge classes of the tetrahedra is equal to the number of tetrahedra.

7.1 Incidence and Neumann-Zagier Matrices

Definition 7.1. For a triangulation we define an incidence matrix to be is a matrix whose rows are indexed by the edge classes of the triangulation (these rows appear first in the matrix) as well as by the cusp homology generators (these are meridian and longitude generators labelled as μ and λ , respectively, for each torus component of the boundary. Also they're chosen such that they intersect the edges in the cusp triangulation transversely, and such that the algebraic intersection number for each is 1). For each tetrahedron of the triangulation there are three columns in the matrix labelled a_i, b_i, c_i these correspond to opposite edges on the tetrahedron (the subscript i labels the particular tetrahedron that these opposite edges belong to) [9].

For the edge rows the entries are count the number of a_i -, b_i - and c_i -edges incident with the edge corresponding to the particular row. While for the cusp homology rows count the number of a_i -, b_i - and c_i -edges cut off by μ and λ , with edges to the left counted with +1 and edges to the right counted with -1.

The Neumann-Zagier matrix is then obtain by taking the incidence matrix and replacing the columns a_i, b_i, c_i with two columns found by subtracting the column b_i from the a_i and c_i (note this choice of using the b_i to subtract with is arbitrary and the a_i and c_i could equally have been chosen). Also we form a column vector ν with the same number of rows of the Neumann-Zagier matrix found by subtracting all the coordinates in the c -columns from the vector consisting of 2s for edge rows and 0s for cusp rows.

Also related to these matrices we define the following matrices. Firstly we ignore the rows in the incidence matrix corresponding to the meridian and longitudes of the tori boundary components, then we define the

matrix \bar{A} to be the $n \times n$ matrix obtained by grouping the a_i columns, while \bar{B} is found by grouping the b_i columns and \bar{C} is the group of the c_i columns.

Now in terms of the \bar{A}, \bar{B} and \bar{C} matrices a generalised angle structure is a triple of vectors $\alpha, \beta, \gamma \in \mathbb{R}^n$ which satisfy the equations,

$$\bar{A}\alpha + \bar{B}\beta + \bar{C}\gamma = (2, \dots, 2)^T, \quad \alpha + \beta + \gamma = (1, \dots, 1)^T.$$

Earlier in defining the Neumann-Zagier matrix using the incidence matrix we subtract and replace columns. This process corresponds to a quad Q for T which is a choice of a pair of opposite edges at each tetrahedron. Once a quad-choice Q is made we can eliminate one of the variables $\alpha_i, \beta_i, \gamma_i$ using the relation $\alpha_i + \beta_i + \gamma_i = 1$. So if we continue to remove the β_i variables then we take the b_i columns as our quad-choice corresponding to the b_i opposite edges. Then we define $A = \bar{A} - \bar{B}$, $B = \bar{C} - \bar{B}$ and $\nu = (2, \dots, 2)^T - \bar{B}(1, \dots, 1)^T$, now with these definitions we see that the generalised angle structure condition becomes

$$A\alpha + B\gamma = \nu.$$

The matrix $(A|B)$ is similar to the Neumann-Zagier, except it is missing the cusp rows. Also this matrix encodes the exponents of the gluing equations corresponding to the ideal triangulation T . It should be noted that Neumann-Zagier showed that $(A|B)$ has rank $n - r$ where recall r is the number of boundary components (assuming that all the boundary components are tori). Thus we can choose $n - r$ linearly independent rows of $(A|B)$ [10].

7.2 Evaluation of the 3D Index

7.2.1 3D Index With no Peripheral Curves

Let M be a 3-manifold with a r tori boundary components with an ideal triangulation T made up of n tetrahedra and no boundary peripheral curves. Note when there are no peripheral curves this corresponds to the evaluation of the 3D at $\mathbf{0}$.

Then we obtain the incidence and Neumann-Zagier matrices. From these matrices can define the matrices $\bar{A}, \bar{B}, \bar{C}$ and then from these we calculate A and B . We denote the columns of $\bar{A}, \bar{B}, \bar{C}$ by $\bar{\mathbf{a}}_j, \bar{\mathbf{b}}_j$ and $\bar{\mathbf{c}}_j$, respectively.

Definition 7.2. The 3D index of M is [4],

$$I_T(\mathbf{0}) = \sum_{\mathbf{k} \in \mathbb{Z}^{n-r} \subset \mathbb{Z}^n} q^{\sum_i k_i} \prod_{j=1}^n J_\Delta(\bar{\mathbf{a}}_j \cdot \mathbf{k}, \bar{\mathbf{b}}_j \cdot \mathbf{k}, \bar{\mathbf{c}}_j \cdot \mathbf{k}).$$

Note in the above the summation vector \mathbf{k} only $n - r$ non-zero entries and the position of these each of these non-zero entries corresponds to the position of one of the $n - r$ linearly independent rows of the matrix $(A\bar{B})$.

7.2.2 Evaluation for a Single Torus Boundary Component With Peripheral Curves

Let M be a 3-manifold with a single torus boundary component, an ideal triangulation T made up of n tetrahedra and let $\bar{\omega}$ be an oriented simple closed curve in ∂M which is in normal form with respect to induced triangulation

$T_{\partial M}$ of ∂M . The 3D index depends only on the homology class of $\bar{\omega}$ [8]. Therefore if we depend the meridian as μ and longitude as λ , then we can represent $\bar{\omega}$ as $\bar{\omega} = x\mu + y\lambda$ where $x, y \in \mathbb{Z}$.

We denote the cusp homology columns of the incidence matrix by a_j, b_j and c_j . Then we define

$$\mathbf{a}_j = (x, y) \cdot a_j,$$

$$\mathbf{b}_j = (x, y) \cdot b_j,$$

and

$$\mathbf{x}_j = (x, y) \cdot c_j.$$

Now our definition of the 3D index becomes [4],

Definition 7.3.

$$I_T(x, y) = \sum_{\mathbf{k} \in \mathbb{Z}^{n-1} \subset \mathbb{Z}^n} q^{\sum_i k_i} \prod_{j=1}^n J_{\Delta}(\bar{\mathbf{a}}_j \cdot \mathbf{k} + \mathbf{a}_j, \bar{\mathbf{b}}_j \cdot \mathbf{k} + \mathbf{b}_j, \bar{\mathbf{c}}_j \cdot \mathbf{k} + \mathbf{c}_j).$$

7.2.3 Evaluation for Multiple Tori Boundary Components With Peripheral Curves

Let M be a 3-manifold with a r tori boundary components which we label as T_1^2, \dots, T_r^2 , and let $\bar{\omega} = (\bar{\omega}_1, \dots, \bar{\omega}_r)$ where $\bar{\omega}_i$ is an oriented multi-curve on T_i^2 . Also T be an ideal triangulation made up of n tetrahdra.

If we let the meridian and longitude of the boundary component T_i^2 be given by μ_i and λ_i , respectively. Then we can represent $\bar{\omega}$ as $\bar{\omega} = \sum_{i=1}^r x_i \mu_i + y_i \lambda_i$. Again we denote the cusp homology columns of the incidence matrix by a_j, b_j and c_j . Then we define

$$\mathbf{a}_j = (x_1, y_1, \dots, x_r, y_r) \cdot a_j,$$

$$\mathbf{b}_j = (x_1, y_1, \dots, x_r, y_r) \cdot b_j,$$

and

$$\mathbf{x}_j = (x_1, y_1, \dots, x_r, y_r) \cdot c_j.$$

Now our definition of the 3D index becomes [4],

Definition 7.4.

$$I_T(x_1, y_1, \dots, x_r, y_r) = \sum_{\mathbf{k} \in \mathbb{Z}^{n-1} \subset \mathbb{Z}^n} q^{\sum_i k_i} \prod_{j=1}^n J_{\Delta}(\bar{\mathbf{a}}_j \cdot \mathbf{k} + \mathbf{a}_j, \bar{\mathbf{b}}_j \cdot \mathbf{k} + \mathbf{b}_j, \bar{\mathbf{c}}_j \cdot \mathbf{k} + \mathbf{c}_j).$$

7.3 Example Calculations

For this project we had a goal writing a MATLAB program which could be inputted the incidence matrix for some 3-manifold along with the integers to be inputted into the 3D index, and this program would return the 3D index. The code can be found in the appendix and we succeeded in this goal for 3-manifolds with single torus boundary components, however it would be difficult to further generalise this code for n number of tori boundaries. The following two example are of 3-manifolds which could be calculated using our MATLAB code.

7.3.1 Figure-8 Knot

The figure-8 knot complement has a single torus boundary component [5]. We can employ the computational software program SnapPy to give the incidence matrix for the figure-8 knot.

$$\begin{array}{l} \text{edge class 1} \\ \text{edge class 2} \\ \mu \\ \lambda \end{array} \begin{array}{c} a_1 \quad b_1 \quad c_1 \quad a_2 \quad b_2 \quad c_2 \\ \left[\begin{array}{cccccc} 2 & 1 & 0 & 2 & 1 & 0 \\ 0 & 1 & 2 & 0 & 1 & 2 \\ 1 & 0 & 0 & 0 & 0 & -1 \\ 1 & 1 & 1 & 1 & -1 & -3 \end{array} \right] \end{array}$$

From the incidence matrix we calculate the matrix $(A|B)$ described earlier.

$$\begin{array}{c} a_1-b_1 \quad c_1-b_1 \quad a_2-b_2 \quad c_2-b_2 \\ \left[\begin{array}{cccc} 1 & -1 & 1 & -1 \\ -1 & 1 & -1 & 1 \end{array} \right] \end{array}$$

Earlier found an ideal triangulation for the figure-8 knot complement which was made up of two ideal tetrahedra and we know that there is a single boundary component, hence we would expect that the number of linearly independent rows in the above matrix is $2 - 1 = 1$, which there clearly is.

So for our summation variable $\mathbf{k} = (k_1, k_2) \in \mathbb{Z} \subset \mathbb{Z}^2$ the only non-zero entry will be the first element, which corresponds to choosing the first row as the row in the set of linearly independent rows making up the matrix.

Hence if we have some peripheral curve given by $\omega = x\mu + y\lambda$, then the 3D index is given by

$$I_{\text{Fig-8 knot}}(x, y) = \sum_{\mathbf{k} \in \mathbb{Z} \subset \mathbb{Z}^2} q^{k_1} J_{\Delta}(2k_1 + x + y, k_1 + y, y) J_{\Delta}(2k_1 + y, k_1 - y, -x - 3y).$$

Using the MATLAB code we can evaluate the above for integers x and y , for example taking both to be zero gives,

$$I_{\text{Fig-8 knot}}(0, 0) = 1 - 2q - 3q^2 + 2q^3 + 8q^4 + \dots$$

7.3.2 5_2 Knot

Again this knot complement has a single torus boundary and using SnapPy gives the incidence matrix,

$$\begin{pmatrix} 1 & 0 & 1 & 1 & 2 & 0 & 1 & 0 & 1 \\ 0 & 1 & 1 & 0 & 0 & 2 & 0 & 1 & 1 \\ 1 & 1 & 0 & 1 & 0 & 0 & 1 & 1 & 0 \\ -1 & 0 & 0 & 0 & 0 & 1 & 0 & 0 & 0 \\ 2 & 0 & -3 & 1 & 0 & -2 & 0 & 0 & 1 \end{pmatrix}.$$

Then calculating the Neumann-Zagier matrix gives,

$$\begin{pmatrix} 1 & 1 & -1 & -2 & 1 & 1 \\ -1 & 0 & 0 & 2 & -1 & 0 \\ 0 & -1 & 1 & 1 & 0 & -1 \\ -1 & 0 & -1 & -1 & 0 & 0 \\ 2 & -3 & 2 & 2 & 0 & 1 \end{pmatrix}.$$

Ignoring the cusp homology rows in the Neumann-Zagier matrix gives,

$$\begin{pmatrix} 1 & 1 & -1 & -2 & 1 & 1 \\ -1 & 0 & 0 & 2 & -1 & 0 \\ 0 & -1 & 1 & 1 & 0 & -1 \end{pmatrix}.$$

There are two linearly independent rows in the above matrix, namely the first and second rows. So we take the summation variable $\mathbf{k} = (k_1, k_2, 0)$ and for some peripheral curve $x\mu + y\lambda$ we find,

$$I_{5,2}(x, y) = \sum_{\mathbf{k} \in \mathbb{Z}^2 \subset \mathbb{Z}^3} q^{k_1+k_2} J_{\Delta}(k_1 - x + 2y, k_2, k_1 + k_2 - 3y) J_{\Delta}(k_1 + y, 2k_1, 2k_2 + x - 2y) J_{\Delta}(k_1, k_2, k_1 + k_2 + y).$$

Again if we take both x and y to be zero (corresponding to the case when there are no peripheral curves) we find,

$$I_{5,2}(0, 0) = 1 - 4q - q^2 + 16q^3 + 26q^4 + \dots$$

8 Discussion and Conclusion

The main goal of this report was to develop sufficient prerequisites to calculate the 3D index for knot complements with r tori boundary components and some peripheral curve. In doing so we gave a general method for finding ideal triangulations of 3-manifolds and along with the hyperbolic geometry required to consider geometric triangulations and how the gluing equations arise, which describe the manner in which the ideal tetrahedra with hyperbolic structure are glued such that the triangulation induces a hyperbolic on the manifold.

From these this we introduced the tetrahedron index and gave a definition of the 3D index in terms of the tetrahedron index using the incidence and Neumann-Zagier matrix. We also calculated the 3D index for the figure-8 knot and 5_2 knot complements, which are both knot complement with a torus boundary, as we wrote a MATLAB program which when inputted the incidence matrix and peripheral curve would output the 3D index. Note this function is limited to 3-manifolds with a single torus boundary component.

An obvious avenue for further work is develop this MATLAB function such that it could handle 3-manifolds with any number of tori boundary components. But more fundamentally there are many more areas of research relating to the 3D index. For example in our work presented here we were considering the 3D index for open 3-manifolds (namely knot complements) which the 3D index can also be defined for closed 3-manifolds (which can be found from knot complements by performing Dehn fillings) [11]. Out of this work has further conjectures arisen, one such conjecture proposed by Gang states that from the 3D index for closed manifolds we can identify

whether the 3-manifold is hyperbolic or not. So further work could be done coding the calculations required to try and verify whether this conjecture holds for known hyperbolic and non-hyperbolic 3-manifolds, as well as working towards a potential proof of the conjecture.

References

- [1] Wikipedia, The Free Encyclopedia 2022, Knot theory, Wikipedia, The Free Encyclopedia, viewed 21 February 2023, https://en.wikipedia.org/wiki/Knot_theory
- [2] Dimofte, T, Gaiotto, D & Gukov, S 2011, ‘3-Manifolds and 3d Indices’, *Adv. Theor. Math. Phys.*, vol. 17, no. 5, pp. 975-1076.
- [3] Garoufalidis, S 2012, ‘The 3d Index of an Ideal Triangulation and Angle Structures’, *The Ramanujan Journal*, vol. 40, pp. 573-604.
- [4] Garoufalidis, S, Hodgson, CD, Rubinstein, JH & Segerman, H 2015, ‘1-Efficient Triangulations and the Index of a Cusped Hyperbolic 3-Manifold’, *Geometry & Topology*, vol. 19, no. 5, pp. 2619-2689.
- [5] Purcell, J.S. and ProQuest (2020) *Hyperbolic knot theory*.
- [6] MENASCO, W. 1983. Polyhedral representation of link complements. *AMS Contemporary Math.*, 20, 305-325.
- [7] Thurston, WP 2002, *The Geometry and Topology of Three-Manifolds*, Mathematical Sciences Research Institute, viewed 20 February 2023, <http://library.msri.org/books/gt3m/PDF/4.pdf>
- [8] Garoufalidis, S., Hodgson, C. D., Hoffman, N. R., & Rubinstein, J. H. (2016). The 3D-index and normal surfaces. *Illinois Journal of Mathematics*, 60(1), 289-352.
- [9] Howie, J.A., Mathews, D.V., Purcell, J.S. and Thompson, E.K., 2021. A-polynomials of fillings of the Whitehead sister. *arXiv preprint arXiv:2106.13462*.
- [10] NEUMANN, W. D. & ZAGIER, D. 1985. Volumes of hyperbolic three-manifolds. *Topology*, 24, 307-332.
- [11] Gang, D 2018, ‘Quantum Approach to Dehn Surgery Problem’, *Geometric Topology*, arXiv: 1803.11143v2

9 Appendix

9.1 Locally Euclidean Requirements.

In the topological category being locally euclidean this means that for every $x \in M$ there exists an open neighbourhood $U \subseteq M$ of x and a homeomorphism $\phi : U \rightarrow V$ where $V \subseteq \mathbb{R}^n$ is open.

In the differential category we have the same condition as in the topological category but we also require that for all of the charts (U_α, ϕ_α) the transitions maps defined $\phi_j \circ \phi_i^{-1} : \phi_i(U_i \cap U_j) \rightarrow \phi_j(U_i \cap U_j)$ to be smooth (specifically C^∞ smooth).

Finally in the piecewise-linear (PL) category we required that for every $x \in M$ there exists an open neighbourhood $U \subseteq M$ of x that is PL homeomorphic to an open set in \mathbb{R}^n . Moreover like in the smooth category

we require that all transition maps to be piecewise-linear maps on polyhedra.

9.2 Equivalence of knots.

Definition 9.1. Two knots (or links) K_1 and K_2 are equivalent if they are ambient isotopic, meaning that there exists a PL or smooth homotopy $h : S^3 \times [0, 1] \rightarrow S^3$ such that $h(\cdot, t) = h_t : S^3 \rightarrow S^3$ is a homeomorphism for each $t \in [0, 1]$ and

$$h(K_1, 0) = h_0(K_1) = K_1,$$

and

$$h(K_2, 1) = h_1(K_2) = K_2.$$

9.3 Polyhedron definition

Definition 9.2. A polyhedron is a closed 3-ball whose boundary is labelled with a finite graph (meaning it has a finite number of vertices and edges) and the complementary regions (which are all simply connected) are called faces.

9.4 Relating Hyperbolic and Riemannian Geometry

Definition 9.3. A Riemannian metric (can sometimes be called a Riemannian structure) of differentiable manifold M is a correspondence which associates to each point $p \in M$ an inner product $\langle \cdot, \cdot \rangle_p$ (a symmetric, bilinear, positive-definite form) on the tangent space $T_p M$.

The Riemannian metric gives us a manner in which to calculate the lengths of vectors tangent to M at p and other quantities such as areas, angles between two curves etc.

Definition 9.4. The first fundamental form (which is often simply defined to be the Riemannian metric) is defined as $\langle v, v \rangle_p$ for $v \in T_p M$.

With these definitions in hand we can turn our attention back to the upper half-plane model. Any point in \mathbb{H}^2 can be given by $x + iy \in \mathbb{R}$ or $(x, y) \in \mathbb{R}^2$ for $y > 0$. With these coordinates we can define the Riemannian metric for any point. For a point $(x, y) \in \mathbb{H}^2$ a tangent vector $v \in T_{(x,y)}\mathbb{H}^2$ which can be written as $v = v_x \frac{\partial}{\partial x} + v_y \frac{\partial}{\partial y}$. Then as a vector we write v as

$$v = \begin{pmatrix} v_x \\ v_y \end{pmatrix}$$

This allows us to define the Riemannian metric on \mathbb{H}^2 as

$$\langle v, w \rangle = \begin{pmatrix} v_x & v_y \end{pmatrix} \begin{pmatrix} \frac{1}{y^2} & 0 \\ 0 & \frac{1}{y^2} \end{pmatrix} \begin{pmatrix} w_x \\ w_y \end{pmatrix}$$

9.5 Definition of Geometric Structure

Definition 9.5. Let X be a manifold and G a group acting on X , then a manifold M has a (G, X) -structure if for every $x \in M$ there exists a chart (U, ϕ) where $U \subset M$ is a neighbourhood of x and $\phi : U \rightarrow \phi(U) \subset X$ is a homeomorphism. With all charts satisfying that if two charts (U, ϕ) and (V, ψ) overlap then the transition map $\gamma = \phi \circ \psi^{-1} : \psi(U \cap V) \rightarrow \phi(U \cap V)$ is an element of G .

9.6 Proof of Equivalence Between the Numbers of Tetrahedra and Edge Classes

Lemma 9.6. Let M be a compact orientable 3-manifold with boundary consisting of r tori. Let T be an ideal triangulation of $\text{int}(M)$ with n ideal tetrahedra, then T has n edge classes.

Proof. It is proven in Hatcher’s Algebraic Topology that since the dimension of M is odd then its Euler characteristic is zero. Thus, if we let V be the number of vertices in the triangulation, E be the number of edges, F be the number of faces and Δ be the number of tetrahedra, then

$$\chi(M) = V - E + F - \Delta = 0.$$

We have that $\Delta = n$ and V since by definition ideal triangulations don’t have vertices (they’re removed), so

$$F - E - n = 0.$$

$$\implies F - n = E.$$

Each tetrahedron in has four faces, but each faces is glued to another face on a different tetrahedron, thus there are $\frac{4n}{2}$ classes of face. Therefore we substitute $F = 2n$ into the above which gives,

$$E = 2n - n = n.$$

□

9.7 Properties of the tetrahedron index I_Δ .

Theorem 9.7. The tetrahedron index satisfies the following linear recursion relations

$$q^{\frac{e}{2}} I_\Delta(m + 1, e) + q^{-\frac{m}{2}} I_\Delta(m, e + 1) - I_\Delta(m, e) = 0.$$

$$q^{\frac{e}{2}} I_\Delta(m - 1, e) + q^{-\frac{m}{2}} I_\Delta(m, e - 1) - I_\Delta(m, e) = 0.$$

$$I_\Delta(m, e + 1) + (q^{e+\frac{m}{2}} - q^{-\frac{m}{2}} - q^{\frac{m}{2}}) I_\Delta(m, e) + I_\Delta(m, e - 1) = 0.$$

$$I_\Delta(m + 1, e) + (q^{-\frac{e}{2}-m} - q^{-\frac{e}{2}} - q^{\frac{e}{2}}) I_\Delta(m, e) + I_\Delta(m - 1, e) = 0.$$

Theorem 9.8. The tetrahedron index satisfies the following duality identity,

$$I_\Delta(m, e) = I_\Delta(-e, -m).$$

Theorem 9.9. *The tetrahedron index satisfies the following triality identity,*

$$I_{\Delta}(m, e) = (-q^{\frac{1}{2}})^{-e} I_{\Delta}(e, -e - m) = (-q^{\frac{1}{2}})^m I_{\Delta}(-e - m, m).$$

Theorem 9.10. *The tetrahedron index satisfies the following pentagon identity,*

$$I_{\Delta}(m_1 - e_2, e_1) I_{\Delta}(m_2 - e_1, e_2) = \sum_{e_3 \in \mathbb{Z}} I_{\Delta}(m_1, e_1 + e_3) I_{\Delta}(m_2, e_2 + e_3) I_{\Delta}(m_1 + m_2, e_3).$$

Theorem 9.11. *The tetrahedron index satisfies the following quadratic identity,*

$$\sum_{e \in \mathbb{Z}} I_{\Delta}(m, e) I_{\Delta}(m, e + c) q^e = \delta_{c,0}.$$

Theorem 9.12. *The minimum degree $\delta(m, e)$ of $I_{\Delta}(m, e)$ is given by,*

$$\delta(m, e) = \frac{1}{2}(m_+(m + e)_+ + (-m)_+ e_+ + (-e)_+ (-e - m)_+ + \max\{0, m, e\}).$$

9.8 Proof of the Invariance of J_{Δ} under S_3 .

Theorem 9.13. *$J_{\Delta}(a, b, c)$ is invariant under S_3 .*

Proof. Let $\sigma \in S_3$ be an arbitrary permutation of $\{a, b, c\}$ so it's an injective function $\sigma : \{a, b, c\} \rightarrow \{a, b, c\}$. Then $J_{\Delta}(a, b, c)$ is invariant under S_3 if $J_{\Delta}(\sigma(a), \sigma(b), \sigma(c)) = J_{\Delta}(a, b, c)$. Consider,

$$J_{\Delta}(\sigma(a), \sigma(b), \sigma(c)) = (-q^{\frac{1}{2}})^{-\sigma(a)} I_{\Delta}(\sigma(a) - \sigma(b), \sigma(c) - \sigma(a)).$$

Note the above uses the third equality in the definition of J_{Δ} . Given that σ is injective we have that either $J_{\Delta}(\sigma(a), \sigma(b), \sigma(c))$ can be seen to be equal to one of the three equalities for $J_{\Delta}(a, b, c)$ directly by substitution, and since $|S_3| = 3! = 6$ this corresponds to three possibilities for σ . Therefore there are another three possibilities for σ where it cannot be seen that $J_{\Delta}(\sigma(a), \sigma(b), \sigma(c)) = J_{\Delta}(a, b, c)$ directly by substitution.

So assume that our σ is in the later case (otherwise our job would already be complete), then

$$J_{\Delta}(a, b, c) = (-q^{\frac{1}{2}})^{-\sigma(a)} I_{\Delta}(\sigma(a) - \sigma(c), \sigma(b) - \sigma(a)).$$

This is due to the fact the three equalities for $J_{\Delta}(a, b, c)$ imply that $J_{\Delta}(a, b, c)$ is equal to an expression of the form $(-q^{\frac{1}{2}})^{-\sigma(a)} I_{\Delta}(\sigma(a) - x, y - \sigma(a))$ where $x \neq y$ and so there are two possible cases either $x = \sigma(b)$ and $y = \sigma(c)$, or $x = \sigma(c)$ and $y = \sigma(b)$. But we have assumed that the definition of $J_{\Delta}(\sigma(a), \sigma(b), \sigma(c))$ is not equal to any of the three equalities for $J_{\Delta}(a, b, c)$ hence the first case not be true, and so we have that $x = \sigma(c)$ and $y = \sigma(b)$.

Now by the duality identity,

$$I_{\Delta}(\sigma(a) - \sigma(c), \sigma(b) - \sigma(a)) = I_{\Delta}(\sigma(a) - \sigma(b), \sigma(c) - \sigma(a)).$$

By substitution of the above into $J_{\Delta}(\sigma(a), \sigma(b), \sigma(c))$ we have,

$$J_{\Delta}(\sigma(a), \sigma(b), \sigma(c)) = (-q^{\frac{1}{2}})^{-\sigma(a)} I_{\Delta}(\sigma(a) - \sigma(c), \sigma(b) - \sigma(a)).$$

Thus we have proven that

$$J_{\Delta}(\sigma(a), \sigma(b), \sigma(c)) = J_{\Delta}(a, b, c).$$

□

```

1 function [result]=NZmatrix(incMatrix)
2 % Calculates the Neumann-Zagier matrix from the inputted incidence matrix.
3 t = width(incMatrix)-(width(incMatrix)/3);
4 result = zeros(height(incMatrix),t);
5 for i=1:t
6     if rem(i,2)==1
7         result(:,i)=incMatrix(:,i + floor(i/2))-incMatrix(:,i + floor(i/2)+1);
8     else
9         result(:,i)=incMatrix(:,i + floor(i/2))-incMatrix(:,i + floor(i/2)-1);
10    end
11 end
12 result;
13 end

```

```

1 function [index]=threeonecomponentindex(y,x,n,incMatrix,tetMatrix)
2 % Calculates the 3d index for any knot complement where
3 % the boundary has one torus component, along the curve
4 % x*mu+y*lambda. Inputted is the incidence matrix for the
5 % particular knot complement and it sums from -n to n.
6 index=zeros(1,size(tetMatrix,2));
7 incMatrixNoCusp = incMatrix(1:height(incMatrix)-2,:);
8 NZmatrixNoCusp = NZmatrix(incMatrixNoCusp);
9 [LINZmatrixNoCusp,LIindices] = licols(NZmatrixNoCusp. ');
10 LIincMatrix = [];
11 for i=1:width(LIindices)
12     LIincMatrix = [LIincMatrix;incMatrix(LIindices(1,i),:)];
13 end
14 LIincMatrix = [LIincMatrix;incMatrix(height(incMatrix)-1,:)];
15 LIincMatrix = [LIincMatrix;incMatrix(height(incMatrix),:)];
16 partitions = [];
17 for i = 0:(2*n)
18     part = integer_partitions(i,height(LIincMatrix)-2);
19     for j = 1:height(part)
20         partitions = [partitions;part(j,:)];
21     end
22 end
23 permutations = [];
24 for i = 1:height(partitions)
25     perm = uniqueperms(partitions(i,:));
26     for j = 1:height(perm)
27         permutations = [permutations;perm(j,:)];
28     end
29 end
30 for i = 1:height(permutations)
31     for j=1:width(permutations)
32         permutations(i,j)=permutations(i,j) - (n/2);
33     end
34 end

```

```

35 for i = 1:height(permutations)
36     term = [1];
37     offset = 0;
38     NegOnePower = 0;
39     for j = 1:3:(width(LIincMatrix)-2)
40         Jinput = [];
41         for k = 0:2
42             entry = 0;
43             for l = 1:(height(LIincMatrix)-2)
44                 entry = entry + (LIincMatrix(l,j+k)*permutations(i,l));
45             end
46             entry = entry + (x*(LIincMatrix(height(LIincMatrix)-1,j+k));
47             entry = entry + (y*LIincMatrix(height(LIincMatrix),j+k));
48             Jinput = [Jinput;entry];
49         end
50         Iinput = [Jinput(1,1) - Jinput(2,1);Jinput(3,1) - Jinput(1,1)];
51         offset = offset + (-1/2)*Jinput(1,1);
52         NegOnePower = NegOnePower - Jinput(1,1);
53         term = conv(term,tetindex(Iinput(1,1),Iinput(2,1),tetMatrix));
54     end
55     for c = 1:length(term)
56         term(1,c) = term(1,c)*(-1)^(NegOnePower);
57     end
58     if (offset < -1)
59         termWithOffset = horzcat(term(2*(-1 - offset):length(term)),zeros(1,2*(-1 - offset)));
60         index=index+termWithOffset(1:length(index));
61     elseif (offset > -1)
62         termWithOffset = horzcat(zeros(1,2*(offset + 1)),term(1:length(term)-(2*(offset + 1))));
63         index=index+termWithOffset(1:length(index));
64     else
65         index=index+term(1:length(index));
66     end
67 end

```